Slow Thermalization Between a Lattice and Free Bose Gas

David C. McKay[1,*] and Brian DeMarco[1]

[1] *Department of Physics, University of Illinois, 1110 W Green St., Urbana, IL 61801*

(Dated: November 21, 2012)

Using a 3D spin-dependent optical lattice, we study thermalization and energy exchange between two ultracold Bose gases, one of which is bound to the lattice and another that is free from the lattice potential. Disruption of inter-species thermalization is revealed through measurements of condensate fraction after the lattice is superimposed on the parabolic confining potential. By selectively heating the lattice-bound species and measuring the rate of heat transfer to the free state, suppression of energy exchange is observed. Comparison with a Fermi's golden rule prediction confirms that this effect is caused by a dispersion mismatch that reduces the phase space available for elastic collisions. This result has critical implications for methods proposed to cool strongly correlated lattice gases.

PACS numbers: 37.10.Jk,37.10.De,03.75.Kk

Ultracold atom gases trapped in optical lattices are an ideal system for exploring strongly correlated quantum matter. Initial work in this area focused on investigating equilibrium phases of Hubbard models, including the realization of the superfluid-to-Mott-insulator phase transition for bosons [1] and the metal-to-Mott-insulator transition for fermions [2, 3]. A new frontier in this field is out-of-equilibrium dynamics; recent results include measurements of quantum quenches [4, 5], expansion dynamics [6], and conduction [7]. These measurements provide insight into phenomena important to material applications, such as transport and diffusion. Understanding strongly correlated dynamics is also critical to developing new techniques for cooling lattice gases. Presently attainable temperatures in optical lattices are too high to observe many phases of interest, such as antiferromagnetism [8]. New methods for cooling are therefore required to reach these low-entropy states.

Here we examine the dynamics most relevant to cooling—thermalization and energy exchange—in a unique strongly correlated system: a fully three-dimensional, species-specific optical lattice [9]. We work with a mixture of two bosonic atomic species, one that is strongly correlated and bound to the lattice, and another weakly interacting state free from the lattice potential. This type of lattice has been proposed as a method for realizing exotic bosonic and fermionic superfluid states [10, 11], a Kondo lattice model [12, 13], and for quantum magnetism [14]. The measurements we present here impact those proposals and suggestions to use this system as a platform for cooling and thermometry of strongly correlated lattice gases. For cooling, a large number of free atoms may be used as a heat reservoir to directly absorb entropy from the lattice gas when it is compressed [15] or to accept entropy via band decay processes [16], while a small impurity of free atoms could be employed for thermometry [9].

There are two methods for realizing species-specific lattices. In one scheme, different atomic species or isotopes are employed, and the relative lattice potential depths are adjusted via the lattice laser wavelength [17, 18]. We use the other technique, which is to employ a mixture of atoms in different hyperfine (i.e., spin) states trapped in a spin-dependent potential [19]. Spin-dependent lattices in 1D have been used to generate entanglement [20], realize quantum walks [21], create atomic impurity disorder [22], and to implement a matter-wave probe [23]. We have used a 3D spin-dependent lattice to create mixed superfluid and Mott insulator phases [9].

We use the $|F = 1, m_F = -1\rangle$ ("$|1\rangle$") and $|F = 1, m_F = 0\rangle$ ("$|0\rangle$") states of ^{87}Rb atoms confined in a 1064 nm crossed-dipole trap with a geometric mean trap frequency (44.5 ± 0.6) Hz; the full details of our apparatus can be found in in Ref. [24]. A mixture of 75×10^3 $|1\rangle$ and 20×10^3 $|0\rangle$ atoms is created from a Bose-Einstein condensate (BEC) of $|1\rangle$ atoms via adiabatic rapid passage (through the $|2, 0\rangle$ state) driven by a microwave-frequency magnetic field. This mixture is miscible in the dipole trap and stabilized against spin-changing collisions by an approximately 10 gauss magnetic field [25]. The atoms are transferred into a spin-dependent cubic lattice by slowing superimposing three orthogonal pairs of counter-propagating, linearly polarized $\lambda = 790$ nm laser beams in a lin-$\perp$-lin configuration (Fig. 1). At this wavelength, the lattice potential depth is proportional to $|m_F|$. Thus, the $|1\rangle$ atoms are lattice-bound and realize the Bose-Hubbard (BH) model, and the $|0\rangle$ atoms do not experience the lattice, as shown in Fig. 1. Using a combination of direct imaging and microwave spectroscopy [25], we confirm that the two species are spatially overlapped on the trap and lattice length scales for all the lattice potential depths explored in this work. Using Kapitza-Dirac diffraction of a BEC in the $|1\rangle$ state, we calibrate the lattice potential depth s, which we express in units of the recoil energy $E_R = 2\hbar^2\pi^2/m\lambda^2$ (where m is the atomic mass).

By measuring condensate fraction, we observe that turning on the lattice disrupts inter-species thermalization. The lattice laser intensity is turned on over 50 ms,

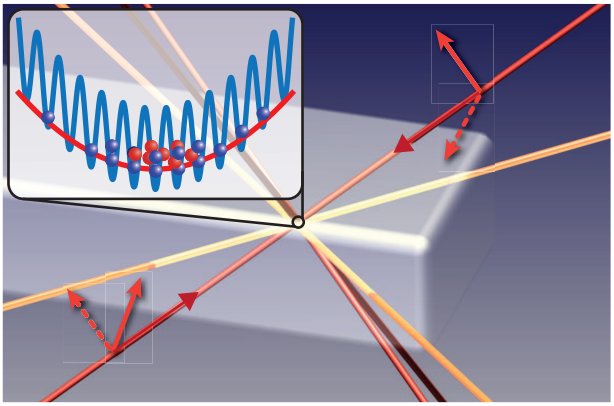

FIG. 1. (Color online) Schematic of the spin-dependent lattice potential. The $|1\rangle$ atoms (blue) are lattice-bound, while the $|0\rangle$ atoms (red) do not experience the lattice potential. Confinement of both species is provided by a 1064 nm crossed-dipole trap (orange lines). The spin-dependent lattice is formed by three pairs of linearly polarized counter-propagating 790 nm laser beams (red lines) with orthogonal polarizations (indicated by dashed arrows); full details of the spin-dependent lattice are given in Ref. [9].

slower than the observed 30 ms inter-species thermalization time in the dipole trap [9]. The lattice modifies the dispersion of the lattice-bound atoms and reduces their kinetic energy, and therefore, if the lattice turn-on is isentropic, the $|1\rangle$ atoms will cool. The temperature of the $|0\rangle$ atoms should likewise decrease if the species remain in thermal equilibrium, and thus condensate fraction N_0/N for that species will increase. We measure N_0/N for each species using time-of-flight imaging as the lattice potential depth s is varied. Separate images of each component are obtained after turning off the lattice and dipole trap and 17–18 ms of time-of-flight; the components are displaced from each other using a magnetic field gradient. Condensate fraction for the $|0\rangle$ atoms is measured using a two-component fit to images, and N_0/N is measured for the $|1\rangle$ atoms using the procedure outlined in Ref. [26]. Before turning on the lattice, the $|0\rangle$-component $N_0/N \approx 0.45$, corresponding to temperature $T \approx 45$ nK.

As shown in Fig. 2, N_0/N for the $|1\rangle$ atoms decreases for higher s, consistent with quantum depletion induced by interactions. In contrast, N_0/N is insensitive to s for the $|0\rangle$ atoms, remaining unchanged from the initial value in the dipole trap across $s = 4$–16. To interpret measured quantities such as N_0/N throughout this work, we use thermodynamic calculations based on site-decoupled mean-field theory (SDMFT) [27, 28] and the local density approximation for the $|1\rangle$ atoms and the semi-ideal model [29] for the $|0\rangle$ atoms. Temperature inferred in this manner from N_0/N is shown in Fig. 2 for both species as s is varied; T for the $|1\rangle$ atoms determined in this manner has an unknown systematic error, since SDMFT does not include all relevant low-energy excitations [30]. The temperature of the $|0\rangle$ atoms remains fixed up to $s = 16$, while the temperature of the $|1\rangle$ atoms decreases by approximately an order of magnitude, indicating that the species are not in equilibrium. The data show a significant deviation from the equilibrium temperature predicted assuming that the lattice turn on is isentropic (solid line in Fig. 2). At all lattice depths, the $|1\rangle$ ($|0\rangle$) temperature is lower (higher) than the equilibrium temperature, consistent with the lattice removing energy from the $|0\rangle$ atoms and suppression of inter-species energy exchange. This measured deviation from the predicted equilibrium temperature for both species indicates that insignificant thermalization occurs on a timescale for which equilibration is nearly complete in the dipole trap.

To quantitatively characterize inter-species thermalization, we selectively heat the $|1\rangle$ atoms and measure the rate of heat transfer $\dot{Q}$ to the $|0\rangle$ component. We choose this approach primarily because interpreting the heat transfer rate requires knowledge of the inter-species temperature difference, which is complicated by the absence of a verified, simple method for measuring the temperature of the $|1\rangle$ atoms at low temperature. In fact, a primary motivation for this work is using the $|0\rangle$ component as a thermometer [9]. While the temperature of the $|0\rangle$ component can be measured straightforwardly, the temperature difference between the two components cannot be controlled as the lattice potential depth is varied without knowledge of T for the $|1\rangle$ atoms.

We overcome this complication by heating the $|1\rangle$ component to infinite kinetic temperature $\widetilde{T}$ with respect to the quasimomentum degree of freedom. Although this may seem to be an unphysical limit, in a single-band lattice system $\widetilde{T} \to \infty$ is well defined. It does not correspond to infinite energy because the kinetic energy is bounded by $4Dt$, where D is the dimensionality and t is the Hubbard tunneling energy. For a three-dimensional multi-band system, such as the lattice in our experiment, we define the $\widetilde{T} \to \infty$ limit as $12t \ll k_B T \ll E_{bg}$, where E_{bg} is the bandgap, and k_B is Boltzmann's constant. In this $\widetilde{T} \to \infty$ limit, all quasimomentum states in the lowest energy band are equally occupied. We use a well-established procedure for generating this configuration—a sequence of rapid increases in s known as dephasing [31]. To dephase, we transiently raise the lattice depth to $s = 20$ three times. Because the $|0\rangle$ component does not experience the lattice potential, the dephasing procedure has no direct effect on their temperature. Images of the $|1\rangle$ atoms after dephasing show that $\widetilde{T} \to \infty$ has been achieved and that the temperature associated with the density distribution is unaffected [25].

To measure the heat transfer rate, we turn on the lattice over 50 ms, dephase the $|1\rangle$ component to infinite $\widetilde{T}$, wait a time $t_{\rm hold}$ for heat to transfer to the $|0\rangle$ component with the atoms held in the lattice and trap, and

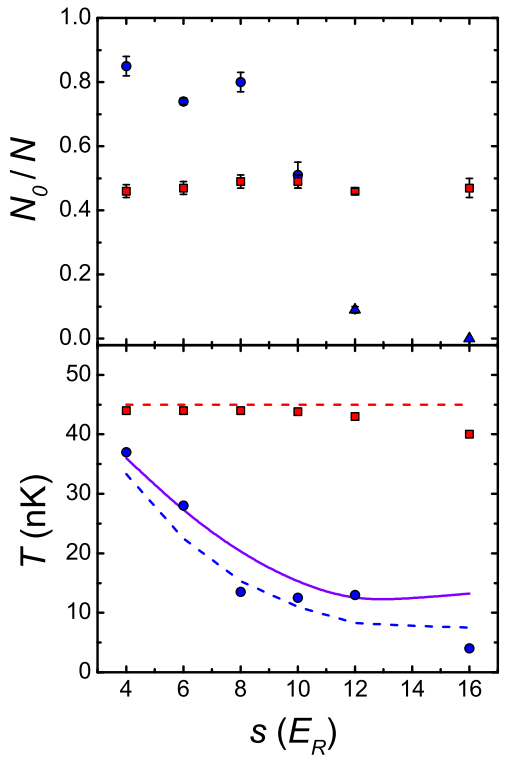

FIG. 2. (Color online) (Top) Condensate fraction versus lattice depth for each species. Blue (red) points are for the $|1\rangle$ ($|0\rangle$) atoms. Each point is averaged over 9–15 experimental runs; the error bars represent the standard error in the mean. For data shown as circles, N_0/N was measured from time-of-flight images obtained after turning off the lattice potential in less than 50 ns. For data shown as triangles, N_0/N was measured after bandmapping the lattice in 100 μs, and therefore these points may overestimate condensate fraction and underestimate temperature [26]. (Bottom) Temperature inferred from the measured N_0/N and number of atoms; the statistical uncertainty T is less than 6%. Mixed Mott insulator and superfluid phases exist (at zero temperature) in the lattice for $s \gtrsim 13$. The lines are predictions assuming that entropy is preserved during the lattice turn on. For the dashed lines, inter-species thermalization is assumed to be absent, and entropy is conserved separately for each component. The predication shown by the solid line assumes inter-species thermal equilibrium.

then measure T for the $|0\rangle$ component using time-of-flight imaging. The rate of change of T for the $|0\rangle$ component $\dot{Q}$, determined by varying $t_{\rm hold}$ at fixed s, is proportional to the rate of inter-species heat exchange. Direct comparison of $\dot{Q}$ between different lattice potential depths is possible since the temperature difference immediately after the dephasing step is independent of s. The temperature for the $|0\rangle$ component after loading the lattice is insensitive to s, and we fix $\widetilde{T} \to \infty$ for the $|1\rangle$ component. Furthermore, since collisions transfer only kinetic energy between species, $\dot{Q}$ is solely sensitive to the kinetic energy degrees of freedom.

Sample data for $s = 4$ are shown in Fig. 3. We observe that T for the $|0\rangle$ component increases linearly in time after the dephasing step for all lattice depths sampled here, which is consistent with the short-time limit of exponential relaxation to equilibrium. We define $\dot{Q}$ as the slope of a linear fit of T for the $|0\rangle$ component vs. $t_{\rm hold}$. To verify this technique, we measure $\dot{Q}$ at different lattice depths without the dephasing step and without the $|1\rangle$ component present. As shown in Fig. 3, $\dot{Q}$ is consistent with zero for these measurements at all s sampled here, demonstrating that any heat transfer observed is induced by dephasing and arises from inter-species interactions.

As shown in Fig. 4, $\dot{Q}$ decreases monotonically with increasing lattice depth and is consistent with zero for $s \gtrsim 12$. Thus, the inter-species thermalization rate is suppressed as the lattice depth increases, in agreement with the disruption of equilibrium evident during turning on the lattice (Fig. 2). While $\dot{Q}$ is expected to decrease with s since the total energy added to the $|1\rangle$ atoms during dephasing is proportional to t (which approximately decreases exponentially with s), energetic arguments cannot explain $\dot{Q}$ disappearing for $s \gtrsim 12$.

We compare the measured $\dot{Q}$ to a Fermi's golden rule (FGR) calculation for the inter-species energy exchange rate. We treat both states as uniform gases occupying a volume V, with the $|1\rangle$ atoms as non-interacting lattice gas at $\widetilde{T} = \infty$ and the $|0\rangle$ atoms as a weakly interacting Bogoliubov Bose gas at $T = 0$. Inter-species energy exchange proceeds via collisions in which a lattice particle of initial quasimomentum $\vec{q}$ scatters from the N-particle condensate at rest into $\vec{q}\,'$ and creates a Bogoliubov excitation of momentum $\vec{p}$. The rate for this process is

$$\Gamma = \frac{2\pi}{\hbar} \left|\langle \vec{q}\,', \vec{p}\,| V_{\rm int} |\, \vec{q}, 0\rangle\right|^2 \delta\left[E(\vec{q}) - E(\vec{q}\,') - \epsilon(p)\right], \quad (1)$$

where $E(\vec{q}) = 2t\sum_{i=1}^{3}\left[1 - \cos(q_i d/\hbar)\right]$ is the energy of the $|1\rangle$ particle in the lattice (i indexes lattice directions), and $\epsilon(p) = \sqrt{(cp)^2 + (p^2/2m)^2}$ is the energy of a Bogoliubov excitation in the $|0\rangle$ gas (c is the speed of sound in the $|0\rangle$ condensate). The interaction $V_{\rm int}$ is the contact interaction for s-wave collisions between ultracold atoms summed over all $N^{(0)}$ $|0\rangle$ condensate particles. The matrix element in Eqn. 1 is $\left|\langle \vec{q}\,', \vec{p}\,| V_{\rm int} |\, \vec{q}, 0\rangle\right|^2 = N^{(0)}\left(\frac{4\pi a\hbar^2}{mV}\right)^2 \frac{p^2}{2m\epsilon(p)}\delta_{\vec{q},\vec{q}\,'+\vec{p}}$, where a is the scattering length and the Kroenecker-delta represents momentum conservation [32, 33]. To calculate the total rate of energy transfer $\dot{E} = N^{(1)}\sum_{\vec{p},\vec{q}}\Gamma\epsilon(p)\rho_{\vec{q}}$ to the $|0\rangle$ atoms, we sum over all final excitation momenta $\vec{p}$ and average over a uniform distribution $\rho_{\vec{q}}$ of initial quasimomenta, where $N^{(1)}$ is the number of $|1\rangle$ atoms in the volume V. Finally, we apply the local-density approximation and integrate over the trapped condensate density profile, and we approximate the $|1\rangle$ density as one particle per site.

In qualitative agreement with the measured $\dot{Q}$, the predicted $\dot{E}$ (dashed line in Fig. 4) decreases with in-

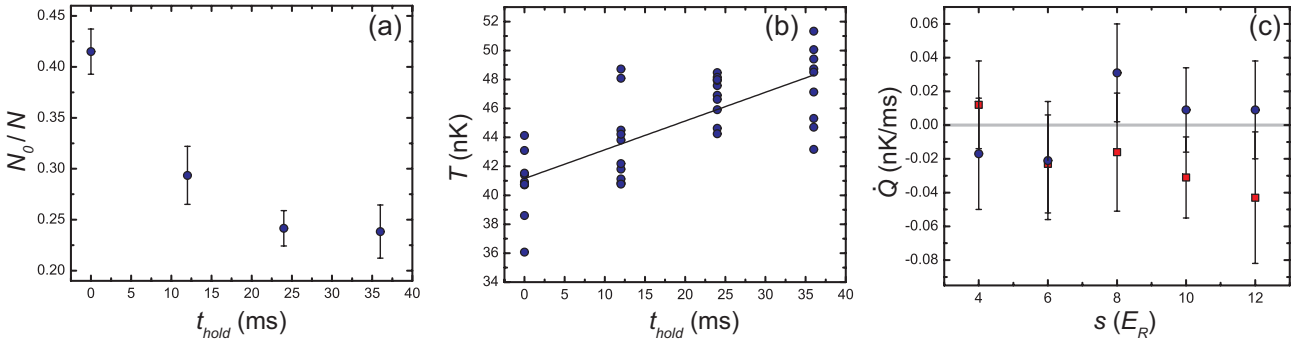

FIG. 3. (Color online) (a) Condensate fraction versus hold time for $s = 4$. Each point is the average of 10 experimental runs, and the error bars show the standard error of the mean. (b) Temperature inferred from the data in (a). The line shows a linear fit, the slope of which is $\dot{Q}$. (c) Control data for the heating rate. The blue circles show $\dot{Q}$ when the lattice atoms are not dephased, and the red squares show $\dot{Q}$ when no lattice atoms are present.

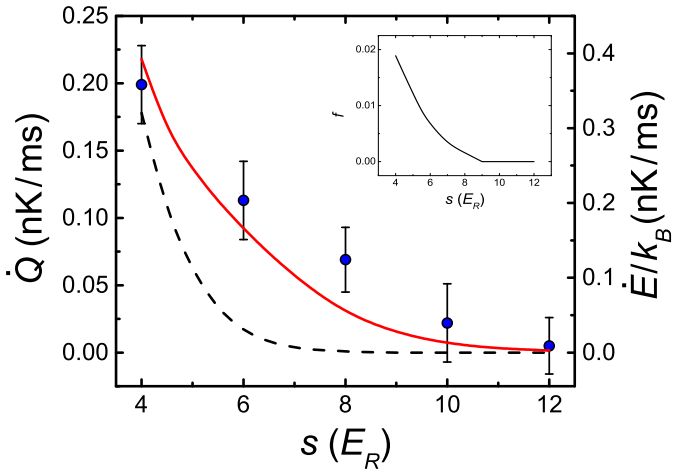

FIG. 4. (Color online) Energy exchange rate for different lattice potential depths, all in the superfluid regime of the BH model. Each point is derived from a fit to data at constant s, such as those shown in Fig. 3a; the error bars are the fit uncertainty. The lines show a FGR calculation of the energy exchange rate $\dot{E}$; the scale has been adjusted so that the rates at $s = 4$ approximately coincide. Averaging over the $|1\rangle$ density profile does not significantly alter these results. For the dashed line, energy is conserved in collisions, while for the solid line the delta-function in Eqn. 1 is replaced by a Gaussian with a standard deviation of U. The inset shows the fraction of phase space f for elastic collisions, which has been averaged over the $|0\rangle$ density distribution.

creasing lattice potential depth and vanishes above a threshold. The essential ingredient in the FGR calculation that gives rise to a threshold lattice depth for thermalization is conservation of energy and momentum in collisions. Since the $|1\rangle$ and $|0\rangle$ atoms have entirely different dispersion relations $E(\vec{q})$ and $\epsilon(p)$, satisfying both energy and momentum conservation can reduce the phase-space of allowed collisions that exchange energy [16]. The inset to Fig. 4 shows the fraction $f = \sum_{\vec{p},\vec{q}} \rho_{\vec{q}}\, \delta\left[E(\vec{q}) - E(\vec{q}\,') - \epsilon(p)\right] \delta_{\vec{q},\vec{q}\,'+\vec{p}} / \sum_{\vec{q}} 1$ of phase space (averaged over the $|1\rangle$ quasimomentum distribution) for elastic collisions, which vanishes for $s \gtrsim 9$. The observation of a threshold in $\dot{Q}$ is strong evidence that dispersion mismatch prevents thermalization between the $|1\rangle$ and $|0\rangle$ gases. The same mechanism is responsible for Kapitza resistance [34], which occurs at interfacial surfaces.

Evident in Fig. 4 is a disagreement between the observed and predicted thresholds. To test if the strong interactions between $|1\rangle$ atoms may be responsible for this discrepancy, we heuristically account for interactions in the FGR calculation by relaxing energy conservation. The solid line in Fig. 4 shows $\dot{E}$ when the δ-function in Eqn. 1 is replaced by a Gaussian with a standard deviation equal to the Hubbard interaction energy U. The close agreement between this case and the measured energy exchange rate suggests that a full understanding of inter-species thermalization will require a more sophisticated treatment of the strong interactions induced by the lattice.

The suppression of energy exchange we observe has critical implications for schemes that rely on fast energy exchange between a lattice and a free-particle bath. Impurity thermometry [9] and cooling methods that require equilibration [15] are problematic, while techniques that rely on thermal isolation may be viable. In particular, our measurements support the feasibility of the cooling technique proposed in Ref. [16], which relies on one-way heat transfer to a free-state bath. Further measurements on dynamics in species-specific optical lattices may also provide new insight into open questions regarding interfacial effects, such as Kapitza resistance.

We acknowledge Erich Mueller and Stefan Baur for suggesting the $\widetilde{T} = \infty$ technique and for initial guidance on the FGR calculation. This work was supported by the DARPA OLE program.

* Now at:Department of Physics, University of Toronto, 60 St. George St., Toronto, ON M5S 1A7, Canada

[1] M. Greiner, O. Mandel, T. Esslinger, T. W. Hänsch, and I. Bloch, Nature **415**, 39 (2002).

[2] R. Jördens, N. Strohmaier, K. Günter, H. Moritz, and T. Esslinger, Nature **455**, 204 (2008).

[3] U. Schneider, L. Hackermüller, S. Will, T. Best, I. Bloch, T. A. Costi, R. W. Helmes, D. Rasch, and A. Rosch, Science **322**, 1520 (2008).

[4] D. Chen, M. White, C. Borries, and B. DeMarco, Phys. Rev. Lett. **106**, 235304 (2011).

[5] M. Cheneau, P. Barmettler, D. Poletti, M. Endres, P. Schausz, T. Fukuhara, C. Gross, I. Bloch, C. Kollath, and S. Kuhr, Nature **481**, 484 (2012).

[6] U. Schneider, L. Hackermller, J. Ronzheimer, S. Will, S. Braun, T. Best, I. Bloch, E. Demler, S. Mandt, D. Rasch, and A. Rosch, Nat. Phys. **8**, 213 (2012).

[7] J.-P. Brantut, J. Meineke, D. Stadler, S. Krinner, and T. Esslinger, Science **337**, 1069 (2012).

[8] D. C. McKay and B. DeMarco, Rep. Prog. Phys. **74**, 054401 (2011).

[9] D. McKay and B. DeMarco, New. J. Phys. **12**, 055013 (2010).

[10] A. B. Kuklov and B. V. Svistunov, Phys. Rev. Lett. **90**, 100401 (2003).

[11] W. V. Liu, F. Wilczek, and P. Zoller, Phys. Rev. A **70**, 033603 (2004).

[12] M. Foss-Feig, M. Hermele, V. Gurarie, and A. M. Rey, Phys. Rev. A **82**, 053624 (2010).

[13] M. Foss-Feig, M. Hermele, and A. M. Rey, Phys. Rev. A **81**, 051603 (2010).

[14] L.-M. Duan, E. Demler, and M. D. Lukin, Phys. Rev. Lett. **91**, 090402 (2003).

[15] T.-L. Ho and Q. Zhou, Proc. Nat. Acad. Sci. **106**, 6916 (2009).

[16] A. Griessner, A. J. Daley, S. R. Clark, D. Jaksch, and P. Zoller, Phys. Rev. Lett. **97**, 220403 (2006).

[17] L. J. LeBlanc and J. H. Thywissen, Phys. Rev. A **75**, 053612 (2007).

[18] J. Catani, G. Barontini, G. Lamporesi, F. Rabatti, G. Thalhammer, F. Minardi, S. Stringari, and M. Inguscio, Phys. Rev. Lett. **103**, 140401 (2009).

[19] I. H. Deutsch and P. S. Jessen, Phys. Rev. A **57**, 1972 (1998).

[20] O. Mandel, M. Greiner, A. Widera, T. Rom, T. W. Hänsch, and I. Bloch, Phys. Rev. Lett. **91**, 010407 (2003).

[21] M. Karski, L. Förster, J.-M. Choi, A. Steffen, W. Alt, D. Meschede, and A. Widera, Science **325**, 174 (2009).

[22] B. Gadway, D. Pertot, J. Reeves, M. Vogt, and D. Schneble, Phys. Rev. Lett. **107**, 145306 (2011).

[23] B. Gadway, D. Pertot, J. Reeves, and D. Schneble, Nature Physics **8**, 544 (2012).

[24] D. McKay, M. White, and B. DeMarco, Phys. Rev. A **79**, 063605 (2009).

[25] See Supplemental Material at [] for information on measurements of spatial overlap and details on dephasing.

[26] S. S. Natu, D. C. McKay, B. DeMarco, and E. J. Mueller, Phys. Rev. A **85**, 061601(R) (2012).

[27] K. Sheshadri, H. R. Krishnamurthy, R. Pandit, and T. V. Ramakrishnan, Europhys. Lett. **257**, 22 (1993).

[28] S. Yoshimura, S. Konabe, and T. Nikuni, Phys. Rev. A **78**, 015602 (2008).

[29] M. Naraschewski and D. M. Stamper-Kurn, Phys. Rev. A **58**, 2423 (1998).

[30] K. V. Krutitsky and P. Navez, Phys. Rev. A **84**, 033602 (2011).

[31] M. Greiner, I. Bloch, O. Mandel, T. W. Hänsch, and T. Esslinger, Phys. Rev. Lett. **87**, 160405 (2001).

[32] F. Zambelli, L. Pitaevskii, D. M. Stamper-Kurn, and S. Stringari, Phys. Rev. A **61**, 063608 (2000).

[33] E. Timmermans and R. Côté, Phys. Rev. Lett. **80**, 3419 (1998).

[34] G. L. Pollack, Rev. Mod. Phys. **41**, 48 (1969).